

Local partial least squares based on global PLS scores

Guanghai Shen^{1,2} | Matthieu Lesnoff^{3,4} | Vincent Baeten² | Pierre Dardenne² |
Fabrice Davrieux^{5,6} | Hernan Ceballos⁷ | John Belalcazar⁷ | Dominique Dufour^{6,7,8,9} |
Zengling Yang¹ | Lujia Han¹ | Juan Antonio Fernández Pierna²

¹College of Engineering, China Agricultural University, Beijing, China

²Food and Feed Quality Unit, Valorisation of Agricultural Products Department, Walloon Agricultural Research Center, Gembloux, Belgium

³CIRAD, UMR SELMET, Montpellier, France

⁴SELMET, Université de Montpellier, CIRAD, INRA, Montpellier Sup Agro, Montpellier, France

⁵UMR Qualisud, CIRAD, Saint-Denis, France

⁶Qualisud, Université de Montpellier, CIRAD, Montpellier SupAgro, Université d'Avignon, Université de La Réunion, Montpellier, France

⁷Cassava Program, International Center for Tropical Agriculture (CIAT), Cali, Colombia

⁸UMR Qualisud, CIRAD, Cali, Colombia

⁹UMR Qualisud, CIRAD, Montpellier, France

Correspondence

Juan Antonio Fernández Pierna, Food and Feed Quality Unit, Valorisation of Agricultural Products Department, Walloon Agricultural Research Center, Gembloux, Belgium.

Email: foodfeedquality@cra.wallonie.be; j.fernandez@cra.wallonie.be

Funding information

China Scholarship Council; HarvestPlus; CIRAD; CIAT

Abstract

A local-based method for near-infrared spectroscopy predictions, the local partial least squares regression on global PLS scores (LPLS-S), is proposed in this work and compared with the usual local PLS (LPLS) regression approach. LPLS-S is based on the idea of replacing the original spectra with a global PLS score matrix before using the usual LPLS. This is done with the aim of increasing the speed of the calculations, which can be an important parameter for online applications in particular, especially when implemented on large databases. In this study, the performance of the two local approaches was compared in terms of efficiency and speed. It could be concluded that the root-mean-square error of prediction of LPLS and LPLS-S were 1.1962 and 1.1602, respectively, but the calculation speed for LPLS-S was more than 20 times faster than for the LPLS algorithm.

KEYWORDS

local calibration, near-infrared spectroscopy, partial least squares, running speed

1 | INTRODUCTION

Near-infrared spectroscopy (NIRS), well known as a fast and nondestructive analytical method, is widely used in combination with partial least squares (PLS) for quality control and shows great potential for application in many fields, such as food (including fruits,¹⁻³ dairy products,⁴ tea,⁵ meat,⁶ fish,⁷ and grain^{8,9}), pharmaceuticals,¹⁰ biomass,¹¹

tobacco,¹² and others. Generally speaking, conventional PLS (global PLS) calibration models can always provide satisfactory results when the relationship between the spectral and reference values is linear and the data are sufficient to cover all possible sources of variability. As Shenk et al suggested,¹³ the samples selected for model construction should include all possible sources of variation in terms of measurement factors (room temperature, operator, and instrument setup) but also in terms of sample population source (origin, process, varieties, storage conditions, and residual moisture), which could increase the robustness of the calibration model. Based on these principles, extensive spectral databases compiling thousands of NIRS absorbance spectra have been created in recent years. In the case of the agricultural sector, the libraries relating to the monitoring of feed, grain, forage, and milk are the most extensive.

However, it is usually observed that the accuracy of the global calibration models (ie, a unique model fitted for all the data set) decreases as complexity of the calibration set increases.^{13,14} To deal with this situation, multiple specific calibrations for samples with a certain chemical composition or source can be developed to improve prediction accuracy, but this can make the modeling process more complex when the categories within the database are very large. In view of these disadvantages, several alternatives based on local regression methods have been proposed. Local approaches can be used to develop individual calibration models for each unknown sample to be predicted by selecting similar spectra from a large spectral library through distance or correlation.^{14,15}

Of the existing local regression methods, comparison analyses using restructured near-infrared and constituent data,¹⁶ locally weighted regression (LWR),¹⁷ and the LOCAL algorithm patented by Shenk et al¹³ are the most widely used when dealing with NIRS applications. Such methods try to deal with nonlinear or clustering problems occurring during global model building. Comparison analyses using restructured near-infrared and constituent, proposed by Davies et al, is a simple and rapid method, which predicts the value of an unknown sample by calculating a weighted average of the analytical reference values of the similar samples, selected based on r^2 between the reduced and modified unknown spectrum and each spectrum in the database, compressed by a Fourier transformation.¹⁶ LWR was introduced by Cleveland and Devlin as a curve-fitting method.¹⁷ It was then adapted for solving nonlinear problems in NIRS calibration models. In particular, Naes et al¹⁸ and Naes and Isaksson,¹⁹ implemented LWR to local principal component regression (PCR) models: for each sample to predict, a neighborhood of calibration samples is selected from a spectral library based on Mahalanobis distances and a different weight is assigned to each calibration sample depending on its distance from the unknown sample. Later, Centner and Massart compared LWR using different regression methods (PCR and PLS), different distance measures (Euclidean and Mahalanobis distance), and different weighting schemes (uniform and cubic weighting) of calibration objects in local models to find an optimal combination.²⁰ The LOCAL algorithm patented by Shenk and Westerhaus is another local regression method, which has been implemented in commercially available software.²¹ In the LOCAL algorithm, correlation coefficients between the spectrum of the unknown sample and those of the available database are calculated instead of Euclidean or Mahalanobis distances. The most similar samples used for the calibration models are selected with reference to a correlation threshold. After the calibration data set has been defined, calibration models are performed by PLS regression.¹³

Besides the above-mentioned methods, there are a few more recent local modeling approaches. Locally biased regression, proposed by Fearn and Davies, uses two criteria to select the most similar spectra to an unknown spectrum from a database: the similarity of predicted values obtained by a global PLSR calibration and the spectral similarity, calculated by the score on the first orthogonal signal correction (OSC) factor in the same way as the PLSR prediction. The samples whose OSC scores lie in an interval around the OSC score defined by the predicted sample will be regarded as similar samples. Samples that pass both similarity tests are then selected as local samples for the new sample to be predicted.²² Another method, the local central algorithm, uses principal component analysis (PCA) and the Mahalanobis distance to select a training set and calculates the final prediction estimate using central tendency statistics such as the mean of the local neighbors for the unknown samples.²³ Local calibration by percentile selection and local calibration by customized radii selection are two novel algorithms for performing local regression based on PLSR that selects samples by establishing a standardized radio around the projection of the unknown sample in the PLS scores space. The unknown sample is then predicted by weighting the regression coefficients and residuals obtained during individual (factor by factor) PLSR models.²⁴

In NIRS applications, all the local approaches, including the above methods, face the problem of long calculation time, in particular when the calibration data set contains a large number of samples. This is a strong constraint for the model calibration abilities (especially when repeated Monte Carlo or bootstrap cross validation has to be implemented²⁵) or for other applications such as online prediction platforms. The long calculation time is due first to the search of the neighbors ("KNN" selection) for each new sample and second to the fact that after each neighborhood selection, a latent variables regression model (eg, PLSR or PCR) is fitted on the original spectral matrix of the neighbors

that is in general very wide. In this article, the approach that we propose for reducing the duration of the second step, and therefore of the overall process, is to fit the local latent variables regression model not on the original spectra of the neighbors but on already compressed data, containing a lower and limited number of columns. We implemented this approach in a local PLSR algorithm, in which the original spectra of each neighborhood were replaced by a matrix of global PLS scores (the compressed data). The method was assessed on a real data set aiming to predict the nutritive quality of the cassava roots in Colombia. The study objectives were to estimate the effects of the preliminary data compression (global PLS scores) in the local PLSR algorithm on the calculation time and the prediction efficiencies.

2 | MATERIAL AND METHODS

2.1 | Data set

Data used in this study for assessing the proposed local method come from a breeding program (Harvest Plus Challenge Program) on cassava plants monitored by the International Center for Tropical Agriculture in Colombia.²⁶ One objective of the program was to study and improve the nutritive quality of the cassava roots (see Davrieux et al²⁶ for details). In particular, NIR spectra of fresh cassava root samples between 2009 and 2013 were recorded in duplicate from 400 to 2498 nm at 2-nm intervals using a FOSS 6500 monochromator with autocup sampling module (FOSS, Hillerod, Denmark), and the carotenoid contents were quantified through HPLC.

The present study focused on the total β -carotene content (TBC). Due to breeding improvements, the mean content of TBC increased slowly from 2009 to 2012, but a significant increase appeared in 2013, by which time the mean was 3 points higher than in 2009,²⁶ as shown in Table 1. Because of an increasing TBC content year after year, Davrieux et al showed the limitation of the usual global PLSR approach and got better predictions using a local PLSR.²⁶

As shown in Figure 1, three types of data sets were built from the original cassava data. Firstly, three calibration data sets, of size $n = 200, 1000,$ and $3000,$ respectively, were built by taking every fifteenth, fourth, and all samples from the samples compiling years 2009 to 2012 ascending in TBC content. The aim of this was to check the influence of the data library size when working with local methods. Secondly, three test sets sampled from the ordered data of year 2013 (each of size $m = 100$) were used for parameter optimization and to assess robustness of the algorithms. Thirdly, the rest of the 2013 dataset (432 samples) were used as independent external set to compare the prediction efficiency of the studied local algorithms.

2.2 | The local prediction algorithms

Two local prediction algorithms were compared (Figure 2): a usual local PLSR (LPLS) and a local PLSR with a preliminary data compression (LPLS-S). It should be noted that the usual local PLSR (LPLS) here was different from the LOCAL algorithm that had been included in the WINISI software package (Infrasoft International, PortMatilda, PA, USA). Let us denote X_r a spectral matrix of a given calibration data set, y_r the corresponding univariate concentration vector, and X_v and y_v , a spectral matrix and a concentration vector, respectively, for a test set to predict. In the study, no pretreatment was applied to the data, but matrices X may be preprocessed without affecting the principle of the methods. The principles of the two algorithms are as follows.

TABLE 1 Descriptive statistics of TBC content (in $\mu\text{g/g}$) for of fresh samples collected from 2009 to 2013

| Year | N | Minimum | Maximum | Mean | SD |
|------|------|---------|---------|------|------|
| 2009 | 572 | 0.70 | 13.40 | 5.10 | 2.30 |
| 2010 | 640 | 0.00 | 14.20 | 6.30 | 2.80 |
| 2011 | 611 | 0.00 | 15.00 | 5.70 | 3.80 |
| 2012 | 1270 | 0.20 | 16.60 | 6.50 | 2.90 |
| 2013 | 732 | 0.20 | 20.10 | 8.10 | 4.10 |

Abbreviation: TBC, total β -carotene content.

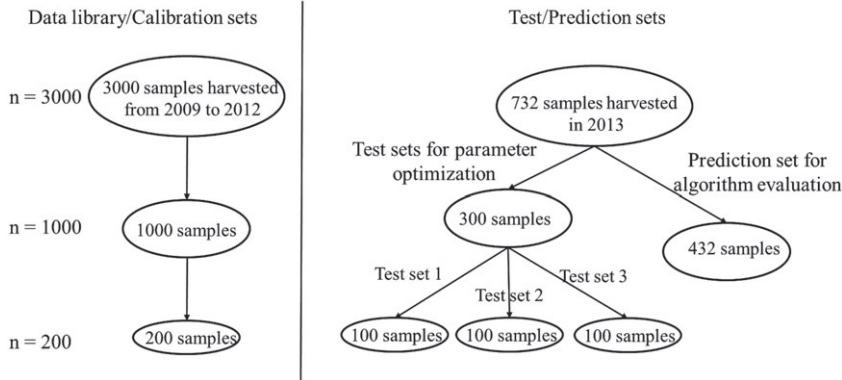


FIGURE 1 Data preparation process

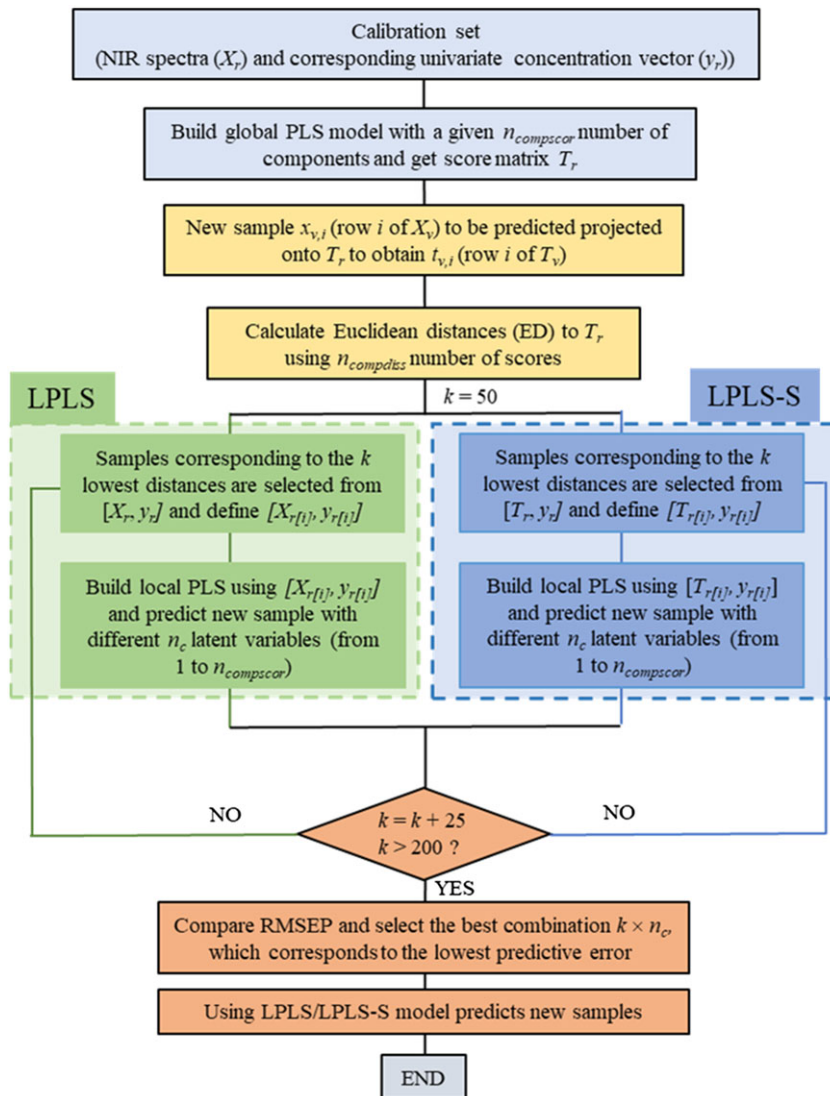


FIGURE 2 Flow chart for local partial least square (LPLS) and local PLS regression on global PLS score (LPLS-S) algorithms

2.2.1 | LPLS

For each new spectrum $x_{v,i}$ (ie, row i of X_v) to be predicted, a number of k nearest neighbors of $x_{v,i}$ are selected in the calibration set, defining the neighborhood $X_{r[i]}$. A PLSR model with a number of n_c components is then fitted over $\{X_{r[i]}, y_{r[i]}\}$ that gives the local prediction for $x_{v,i}$. The neighborhood $X_{r[i]}$ is calculated from compressed data, as follows. A global PLSR model is fitted over $\{X_r, y_r\}$ with a given $n_{\text{comp}}_{\text{score}}$ number of components. This gives the score matrix T_r (with $n_{\text{comp}}_{\text{score}}$ columns) and, by projection of X_v in the T_r score space, the score matrix T_v . Euclidean distances are then

calculated between $t_{v,i}$ (ie, row i of T_v) and all the t_r (ie, rows of T_r) using n_{compdiss} number of scores. The samples corresponding to the k lowest distances are finally selected and define $X_{r[i]}$.

The implementation of this process for all rows of X_v returns the y -prediction vector for the single combination $k \times n_c$. A predictive error estimate, such as root-mean-square error of prediction (RMSEP), is then calculated by comparison with the observed data y_v . The parameters k and n_c can be optimized by defining a discrete grid over k and n_c ²⁰: the predictive error is calculated for each node of the grid, and the node with the lowest predictive error corresponds to the combination finally selected for the predictions. In this study, the grid was set to $\{k = 50, 75, \dots, 200\} \times \{n_c = 1, 2, \dots, 25\}$. The optimization was performed for each of the three test sets (of size $m = 100$) extracted from the 2013 data.

2.2.2 | LPLS-S

In this algorithm, matrices X_r and X_v are first transformed to global PLS score matrices T_r and T_v , with a given n_{compscor} number of components. The above LPLS algorithm is then simply run on T_r and T_v .

2.3 | Model comparison

The calculation time and the predictive efficiency were compared between LPLS and LPLS-S for various values of the parameters n_{compscor} , n_{compdiss} , and n , the size of the data set (ie, number of samples) used for calibrating the algorithms, following a complete experiment design shown in Table 2. Three levels of global PLS scores (n_{compscor} : 3, 10, and 25) used for LPLS-S, three different numbers of scores (n_{compdiss} : 3, 10, and 25) used for calculating distances, and three different sizes for building the calibration data set ($n = 200, 1000, \text{ and } 3000$) were combined. Predictions were done for each test set (using models developed on the various calibration sets $n = 200, 1000, \text{ and } 3000$) for the complete grid as shown in Table 2, and a final combination was selected corresponding to the lowest RMSEP in the grid.

TABLE 2 Experimental design for comparing both LPLS and LPLS-S algorithms

| Scenarios | n_{compscor} | n_{compdiss} | k | n_c | n | m |
|-----------|-----------------------|-----------------------|----------------|--------------|------|-----|
| 1 | 3 | 3 | 50, 75 ... 200 | 1, 2, 3 | 200 | 100 |
| 2 | 10 | 3 | 50, 75 ... 200 | 1, 2, ... 10 | 200 | 100 |
| 3 | 10 | 10 | 50, 75 ... 200 | 1, 2, ... 10 | 200 | 100 |
| 4 | 25 | 3 | 50, 75 ... 200 | 1, 2, ... 25 | 200 | 100 |
| 5 | 25 | 10 | 50, 75 ... 200 | 1, 2, ... 25 | 200 | 100 |
| 6 | 25 | 25 | 50, 75 ... 200 | 1, 2, ... 25 | 200 | 100 |
| 7 | 3 | 3 | 50, 75 ... 200 | 1, 2, 3 | 1000 | 100 |
| 8 | 10 | 3 | 50, 75 ... 200 | 1, 2, ... 10 | 1000 | 100 |
| 9 | 10 | 10 | 50, 75 ... 200 | 1, 2, ... 10 | 1000 | 100 |
| 10 | 25 | 3 | 50, 75 ... 200 | 1, 2, ... 25 | 1000 | 100 |
| 11 | 25 | 10 | 50, 75 ... 200 | 1, 2, ... 25 | 1000 | 100 |
| 12 | 25 | 25 | 50, 75 ... 200 | 1, 2, ... 25 | 1000 | 100 |
| 13 | 3 | 3 | 50, 75 ... 200 | 1, 2, 3 | 3000 | 100 |
| 14 | 10 | 3 | 50, 75 ... 200 | 1, 2, ... 10 | 3000 | 100 |
| 15 | 10 | 10 | 50, 75 ... 200 | 1, 2, ... 10 | 3000 | 100 |
| 16 | 25 | 3 | 50, 75 ... 200 | 1, 2, ... 25 | 3000 | 100 |
| 17 | 25 | 10 | 50, 75 ... 200 | 1, 2, ... 25 | 3000 | 100 |
| 18 | 25 | 25 | 50, 75 ... 200 | 1, 2, ... 25 | 3000 | 100 |

n_{compscor} (only LPLS-S): number of global scores used for local partial least squares (PLS) regression on global PLS scores (LPLS-S); n_{compdiss} : number of scores used for calculating the distances; k : number of nearest neighbors; n_c : number of latent variable for PLS models; n : number of samples in the calibration set; m : number of samples to be predicted.

All the data were processed using Matlab version 7.14 (The Mathworks, Inc., Natick, MA, USA) with the PLS_Toolbox version 8.0 (Eigenvector Research, Wenatchee, WA, USA). Computer configuration: Intel(R) Core (TM) I5-7300HQ, CPU at 2.50 GHz, 8 GB random access memory, and 64-bit operating system.

3 | RESULTS AND DISCUSSION

3.1 | PCA of samples

PCA was first applied to all the raw spectra of cassava samples harvested from 2009 to 2013. As shown in Figure 3, the PCA scores plot gave a cluster trend of different years' cassava samples. All the samples used in this study were clustered into four groups, which was due to the fact that year after year, cassava genotypes with higher dry matter and carotenoid content were obtained by the breeding project, as reported by Davrieux et al.²⁶

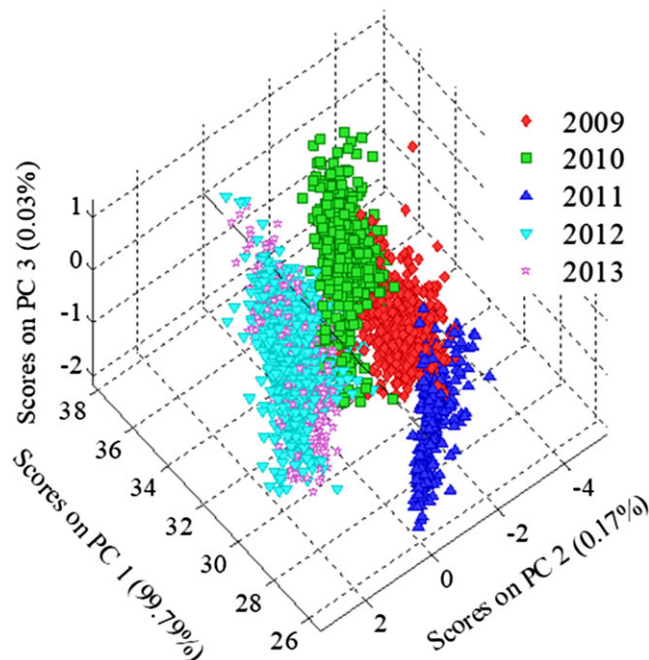


FIGURE 3 Principal component analysis scores plot for cassava samples collected from 2009 to 2013

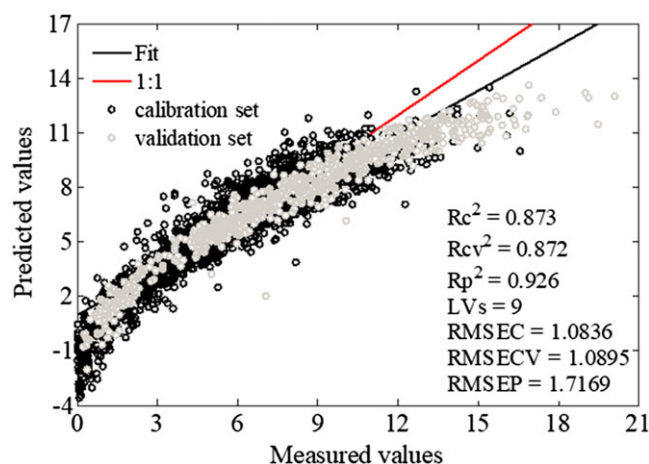


FIGURE 4 Relationship between predicted and measured values of total β -carotene content using a global partial least square method

3.2 | Global PLS regression model

A global PLS regression model was built with samples harvested from 2009 to 2012 (total calibration set of 3000 samples) and used to predict the independent prediction set of 432 samples (samples harvested in 2013). No pretreatment of data has been applied. The results are shown in Figure 4, where it can be seen that the root-mean-square error of calibration and the root-mean-square error of cross validation were 1.084 and 1.089, respectively, meaning that the calibration model was robust. However, a large RMSEP (1.7169) and a small relative percentage deviation (RPD = 2.39, $RPD = SD/RMSEP$) value appeared when new samples harvested in 2013 (gray in Figure 4) were predicted by this model. The RPD is usually used for testing the accuracy of NIRS calibration models, and $RPD > 3$ is considered adequate for analytical purposes for agricultural products.^{27,28} RPD = 2.39 therefore indicated that a global PLSR model

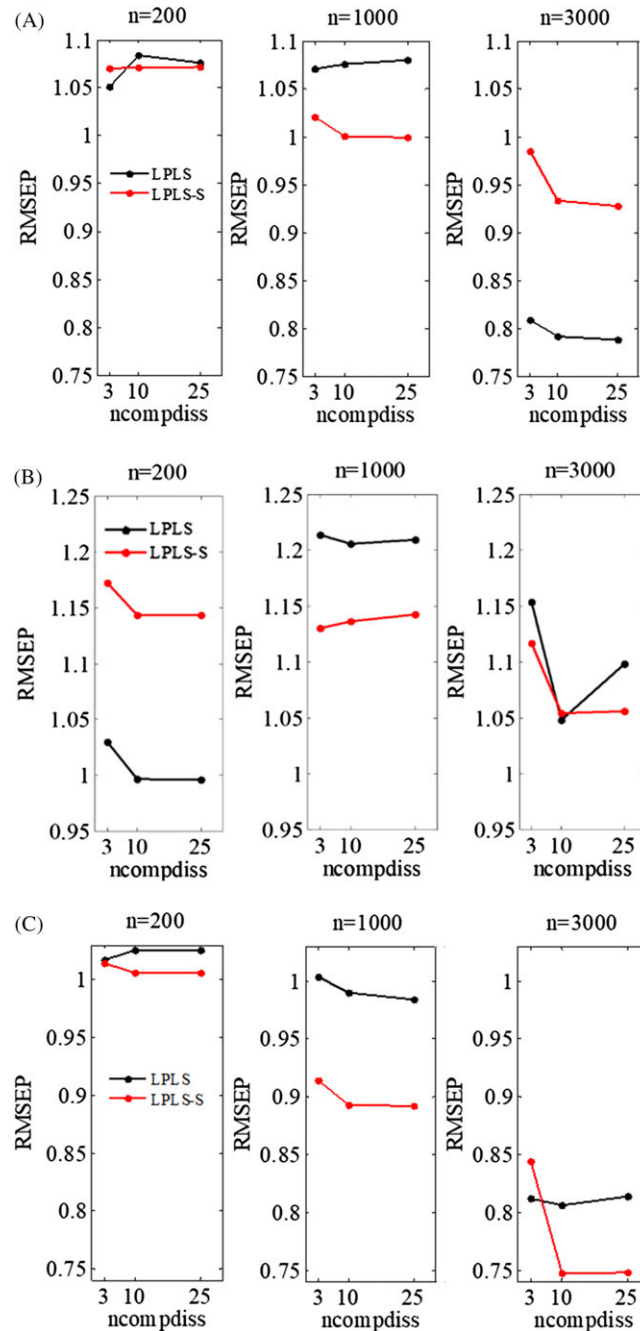


FIGURE 5 Root-mean-square error of prediction (RMSEP) comparison between both local partial least square (LPLS) and local PLS regression on global PLS score (LPLS-S): A, test set 1, B, test set 2, and C, test set 3

failed to properly predict new samples. Moreover, there was a clear nonlinear relationship between measured and predicted values, especially for the higher TBC content, possibly because samples changed with the increasing content of the constituent of interest year after year. In this case, the global PLSR model could not be used for the effective prediction of new harvested samples in 2013.

3.3 | LPLS and LPLS-S algorithms

To address the poor prediction performance as well as the nonlinearity problem when using a global PLSR model, the two different locally based PLS regression algorithms (LPLS and LPLS-S) were used and compared.

3.3.1 | Parameter optimization results for LPLS and LPLS-S

The LPLS-S algorithm was proposed for accelerating the prediction process based on global PLS scores. The running times and efficiency of both LPLS and LPLS-S algorithms were compared on the three test sets. The results are displayed in Tables S1 and S2 and Figure 5. All the results were acquired under the optimum combination of k and n_c corresponding to the lowest RMSEP of the scenarios in Table 2 and for 25 global PLS scores when LPLS-S was used. As observed, the RMSEP values for LPLS show no distinct rule as the size of the calibration data (n) gets larger, but the running time increases significantly from 3.57 to 6.42 seconds. Unlike with the LPLS algorithm, the prediction precision for LPLS-S increased with n , while the calculating time remained basically unchanged. On average, when using 200, 1000, and 3000 calibration samples, the LPLS-S algorithm was 13.04, 14.43, and 21.66 times faster than the LPLS method, respectively. This means that the more calibration samples there are in the calibration data set, the more obvious the advantage in running time for the LPLS-S algorithm, with similar prediction performance. Besides, when the same calibration data set is used, the number of scores used for calculating distance (n_{compdiss}) has a very low effect on the running time of both LPLS and LPLS-S algorithms but has a great impact on the prediction results.

Besides the size of the calibration data set and the number of scores used for distance calculation, the effect of the scores extracted from global PLSR models ($n_{\text{compsscor}}$) on the running time of the LPLS-S algorithm was also studied. As shown in Table 2, three $n_{\text{compsscor}}$ values (3, 10, and 25) were extracted and used for LPLS-S models based on different sizes of calibration data. The results are shown in Table 3 and Figure 6. It can be seen that if the number of extracted scores is too few, the calculating speed is faster (Figure S1), but the prediction becomes inefficient (Table 3 and Figure 6A to 6c). However, when the same number of scores is used for the distance calculation under the same data library, the prediction accuracy increases with the number of global PLS scores used for LPLS-S

TABLE 3 RMSEP for LPLS-S using different numbers of global PLS scores and different numbers of scores for distance calculation

| Test set | n_{compdis} $n_{\text{compsscor}}$ | n=200 | | | n=200 | | | n=200 | | |
|------------|--|--------|--------|--------|--------|--------|--------|--------|--------|--------|
| | | 3 | 10 | 25 | 3 | 10 | 25 | 3 | 10 | 25 |
| Test set 1 | 3 | 2.4237 | - | - | 2.4572 | - | - | 2.5179 | - | - |
| | 10 | 1.0948 | 1.0927 | - | 1.0462 | 1.0330 | - | 1.0113 | 0.9461 | - |
| | 25 | 1.0700 | 1.0711 | 1.0717 | 1.0212 | 1.0006 | 0.9991 | 0.9853 | 0.9338 | 0.9278 |
| Test set 2 | 3 | 2.3818 | - | - | 2.4305 | - | - | 2.5677 | - | - |
| | 10 | 1.1904 | 1.1585 | - | 1.1319 | 1.1390 | - | 1.1353 | 1.0737 | - |
| | 25 | 1.1721 | 1.1431 | 1.1432 | 1.1302 | 1.1364 | 1.1423 | 1.1165 | 1.0539 | 1.0556 |
| Test set 3 | 3 | 2.3604 | - | - | 2.3905 | - | - | 2.4886 | - | - |
| | 10 | 1.0435 | 1.0421 | - | 0.9366 | 0.9226 | - | 0.8642 | 0.7684 | - |
| | 25 | 1.0142 | 1.0062 | 1.0062 | 0.9143 | 0.8928 | 0.8919 | 0.8438 | 0.7475 | 0.7478 |

$n_{\text{compsscor}}$ (only LPLS-S): number of global scores used for local partial least squares (PLS) regression on global PLS scores (LPLS-S); n_{compdiss} : number of scores used for calculating the distances; n : number of samples in the calibration set; RMSEP: root-mean-square error of prediction.

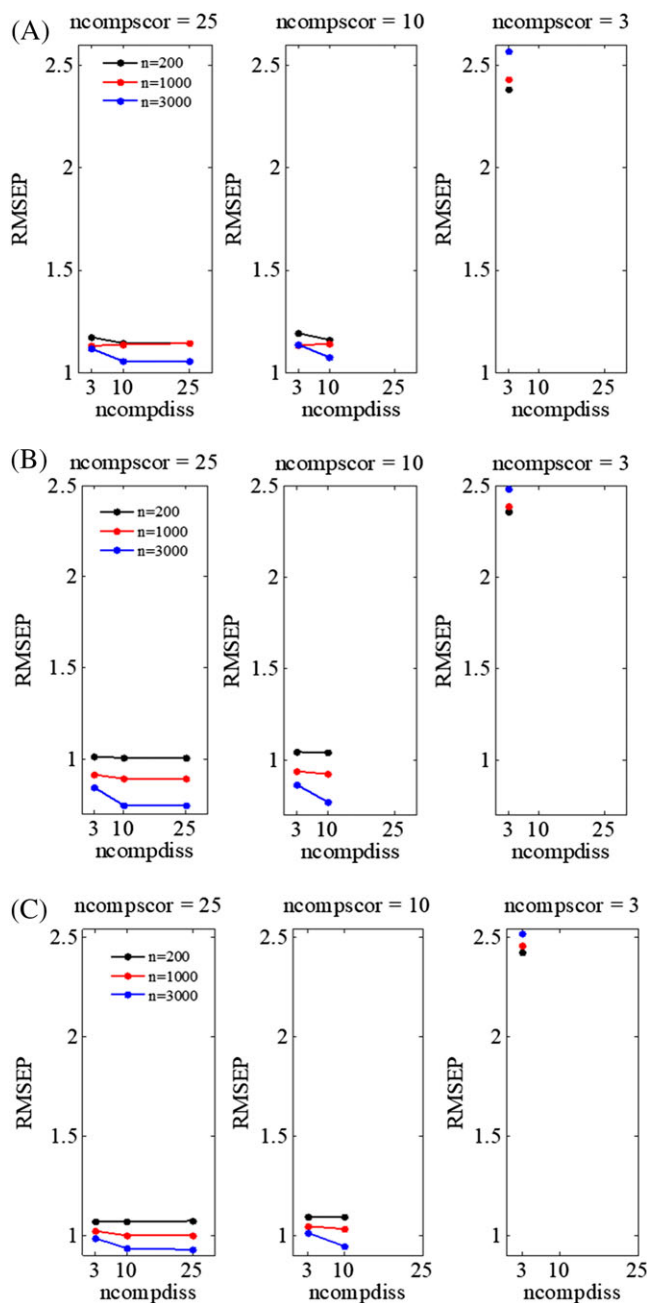


FIGURE 6 The effects of the number of global partial least square scores on root-mean-square error of prediction (RMSEP) for A, test set 1, B, test set 2, and C, test set 3

models. In summary, if a more precise prediction result is needed with the LPLS-S algorithm, 25 global PLS scores and 10 or 25 scores for distance calculation are the proper parameter selections; if a faster prediction speed with satisfactory results is needed, 10 global PLS scores and 10 scores for distance calculation are the best combination.

Three independent test sets were used for parameter optimization, which is an important step for both LPLS and LPLS-S algorithms. The optimum combination of the size of data library (n), the number of scores for distance calculation (n_{compdiss}), the number of latent variables for PLSR models (n_c), and the number of neighbors (k) corresponds to the minimum RMSEP for each test set (Table 4). It can be seen that when working with LPLS, the optimum parameters differ from one test set to another, which is not the case for LPLS-S where the parameters are rapidly stabilized and are the same whatever the test set. Moreover, the optimum latent variables obtained for LPLS models are too many, which may involve too much noise and can result in overfitting. The number of latent

TABLE 4 The optimum parameters obtained by each test set for LPLS and LPLS-S algorithms

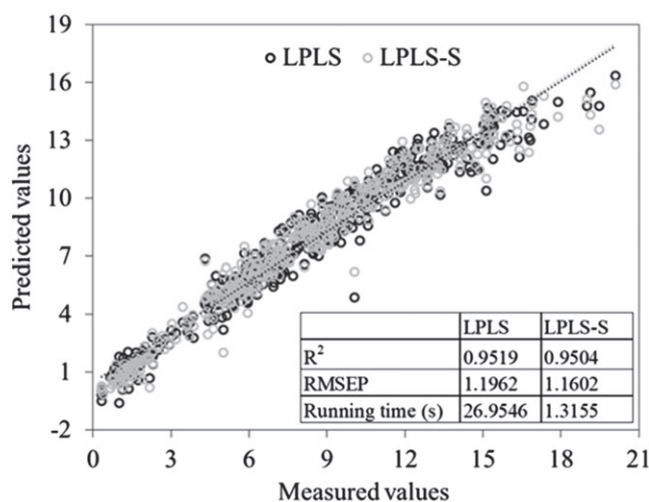
| Algorithm | Parameters | Test Set 1 | Test Set 2 | Test Set 3 |
|-----------|-----------------------|------------|------------|------------|
| LPLS | n | 3000 | 200 | 3000 |
| | n_{compdiss} | 25 | 25 | 10 |
| | n_c | 15 | 14 | 16 |
| | k | 150 | 50 | 175 |
| LPLS-S | n | 3000 | 3000 | 3000 |
| | n_{compdiss} | 25 | 10 or 25 | 10 or 25 |
| | n_c | 5 | 5 | 5 |
| | k | 50 or 75 | 75 | 75 |

n : number of reference samples in calibration set; n_{compdiss} : number of scores used for calculating the distances; n_c : latent variable for partial least squares (PLS) models; k : number of nearest neighbors; LPLS: local PLS; LPLS-S: local PLS regression on global PLS score.

variables used in LPLS-S models decreased to 5 compared with LPLS, which indicates the robustness of the LPLS-S algorithm.

3.3.2 | Performance of LPLS and LPLS-S

In order to obtain good prediction results, the parameters of LPLS and LPLS-S should be defined according to the conclusions in Section 3.3.1. For the LPLS algorithm, 150 nearest neighbors, 25 scores for distance calculation, 15 latent variables, and 3000 reference samples were selected as the optimum combination for predicting new samples harvested in 2013. The results are shown in Figure 7 in black. The prediction process took 26.95 seconds, and the RMSEP decreased from 1.7169 to 1.1962 compared with the global PLSR method, while the RPD increased to 3.43. In the LPLS-S algorithm, 75 nearest neighbors, 25 global PLS scores, 25 scores for distance calculation, 5 latent variables, and 3000 reference samples were used to build local models for predicting samples harvested in 2013. The results compared with the LPLS method are shown in Figure 6 in gray. The RMSEP of the LPLS-S algorithm decreased significantly to 1.1602 compared with the global PLS (1.7169), and the RPD increased to 3.53 (instead of 2.39 for the global PLS), which is similar to the results obtained by LPLS, but the calculation speed was more than 20 times faster than for the LPLS algorithm. By contrast, it can be concluded that the LPLS-S algorithm based on compressed data instead of original spectra is a good method for greatly decreasing computation time and improving computation efficiency without losing prediction accuracy compared with the LPLS algorithm. It can also be observed that the nonlinearity problem was reduced.

**FIGURE 7** Prediction results and scatter plots of measured values vs predicted values for both local partial least square (LPLS) and local PLS regression on global PLS score (LPLS-S) algorithms

4 | CONCLUSION

During the past few decades, a large number of local strategies have been proposed and showed good performance when dealing with nonlinearity problems encountered in global PLSR models. However, with the continuous accumulation of data, the database keeps increasing. This makes local strategies less useful, as the local algorithms need to establish an analysis model for each sample, which requires a long calculation time. In this study, a new local strategy, LPLS-S, based on compressed data (global PLS scores) instead of original spectra, was carefully investigated. The main conclusions derived from this research are that the prediction precision of the LPLS-S algorithm increases when the database becomes larger and that between 10 and 25 global PLS scores are needed depending on the precision prediction/speed ratio needed. Compared with the LPLS algorithm, LPLS-S might lose prediction accuracy in some cases due to the preliminary compression, but the calculation speed is greatly improved, and the more reference samples in the database, the more obvious the running time advantage for LPLS-S. Also, this becomes an important output when working with online prediction systems. Moreover, in this study, the optimum parameters for the LPLS-S algorithm are easier and more repeatable to be obtained whatever the test set than the LPLS algorithm. However, this should be validated on other data sets. It should be mentioned that the local strategies permitted to correct the nonlinearity present in the data.

In summary, all the results indicate that LPLS-S has great potential to deal with huge data. Furthermore, the use of the global PLS scores to compress the original spectra was successfully applied to the local PLS method. The same approach could also be used for any other prediction methods, including support vector machines and neural networks, which have a reputation for being slow techniques.

ACKNOWLEDGEMENTS

This work was supported by the CIAT Cassava Project (Colombia) and CIRAD Qualisud Research Unit (France) and funded mainly by HarvestPlus, c/o IFPRI (www.harvestplus.org), part of the Consultative Group on International Agriculture Research (CGIAR), Program on Agriculture for Nutrition and Health (A4NH), project: “Enhancing the nutritional quality of cassava roots to improve the livelihoods of farmers in marginal agriculture land in Africa, Haiti, and North-Colombia” and the CGIAR Research Program on Roots, Tubers and Bananas (RTB) (www.rtb.cgiar.org), project: “Driving livelihood improvements through demand-oriented interventions for competitive production and processing of RTBs” with support from CGIAR Trust Fund contributors (<https://www.cgiar.org/funders/>). The authors gratefully acknowledge also financial support from the China Scholarship Council that allowed the author to work at the CRA-W.

CONFLICT OF INTEREST

The authors declare no conflict of interest.

ORCID

Guanghui Shen  <https://orcid.org/0000-0002-9900-5586>

REFERENCES

1. Nicolai BM, Beullens K, Bobelyn E, et al. Nondestructive measurement of fruit and vegetable quality by means of NIR spectroscopy: a review. *Postharvest Biol Technol.* 2007;46(2):99-118.
2. Magwaza LS, Opara UL, Nieuwoudt H, Cronje PJR, Saeys W, Nicolai B. NIR spectroscopy applications for internal and external quality analysis of Citrus fruit—a review. *Food Bioproc Tech.* 2012;5(2):425-444.
3. Pissard A, Fernández Pierna JA, Baeten V, et al. Non-destructive measurement of vitamin C, total polyphenol and sugar content in apples using near-infrared spectroscopy. *J Sci Food Agr.* 2013;93(2):238-244.
4. Laporte M, Paquin P. Near-infrared analysis of fat, protein, and casein in cow's milk. *J Agric Food Chem.* 1999;47(7):2600-2605.
5. Chen Q, Zhao J, Chaitep S, Guo Z. Simultaneous analysis of main catechins contents in green tea (*Camellia sinensis* (L.)) by Fourier transform near infrared reflectance (FT-NIR) spectroscopy. *Food Chem.* 2009;113(4):1272-1277.
6. Kapper C, Klont RE, Verdonk JMAJ, Urlings HAP. Prediction of pork quality with near infrared spectroscopy (NIRS). *Meat Sci.* 2012;91(3):294-299.

7. Ru YJ, Glatz PC. Application of near infrared spectroscopy (NIR) for monitoring the quality of milk, cheese, meat and fish. Review. *Asian Austral J Anim.* 2000;7(13):1017-1025.
8. Ferreira DS, Pallone JAL, Poppi RJ. Direct analysis of the main chemical constituents in Chenopodium quinoa grain using Fourier transform near-infrared spectroscopy. *Food Control.* 2015;48:91-95.
9. Zhang C, Shen Y, Chen J, Xiao P, Bao J. Nondestructive prediction of total phenolics, flavonoid contents, and antioxidant capacity of rice grain using near-infrared spectroscopy. *J Agric Food Chem.* 2008;56(18):8268-8272.
10. Roggo Y, Chalus P, Maurer L, Lema-Martinez C, Edmond A, Jent N. A review of near infrared spectroscopy and chemometrics in pharmaceutical technologies. *J Pharm Biomed Anal.* 2007;44(3):683-700.
11. Chadwick DT, McDonnell KP, Brennan LP, Fagan CC, Everard CD. Evaluation of infrared techniques for the assessment of biomass and biofuel quality parameters and conversion technology processes: a review. *Renew Sustain Energy Rev.* 2014;30:672-681.
12. Li Z, Li C, Gao Y, et al. Identification of oil, sugar and crude fiber during tobacco (*Nicotiana tabacum* L.) seed development based on near infrared spectroscopy. *Biomass Bioenergy.* 2018;111:39-45.
13. Shenk JS, Westerhaus MO, Berzaghi P. Investigation of a LOCAL calibration procedure for near infrared instruments. *J Near Infrared Spec.* 1997;5(4):223-232.
14. Berzaghi P, Shenk JS, Westerhaus MO. LOCAL prediction with near infrared multi-product databases. *J Near Infrared Spec.* 2000;8(1):1-9.
15. Godin B, Mayer F, Agneessens R, et al. Biochemical methane potential prediction of plant biomasses: comparing chemical composition versus near infrared methods and linear versus non-linear models. *Bioresour Technol.* 2015;175:382-390.
16. Davies AM, Britcher HV, Franklin JG, Ring SM, Grant A, McClure WF. The application of fourier-transformed near-infrared spectra to quantitative analysis by comparison of similarity indices (CARNAC). *Microchim Acta.* 1988;1-6(94):61-64.
17. Cleveland WS, Devlin SJ. Locally weighted regression: an approach to regression analysis by local fitting. *J Am Stat Assoc.* 1988;83(403):596-610.
18. Naes T, Isaksson T, Kowalski B. Locally weighted regression and scatter correction for near-infrared reflectance data. *Anal Chem.* 1990;62(7):664-673.
19. Næs T, Isaksson T. Locally weighted regression in diffuse near-infrared transmittance spectroscopy. *Appl Spectrosc.* 1992;46(1):34-43.
20. Centner V, Massart DL. Optimization in locally weighted regression. *Anal Chem.* 1998;70(19):4206-4211.
21. Pérez Marín D, Garrido Varo A, Guerrero J. Non-linear regression methods in NIRS quantitative analysis. *Talanta.* 2007;72(1):28-42.
22. Fearn T, Davies AM. Locally-biased regression. *J Near Infrared Spec.* 2003;11(6):467-478.
23. Zamora Rojas E, Garrido Varo A, Van den Berg F, Guerrero Ginel JE, Pérez Marín D. Evaluation of a new local modelling approach for large and heterogeneous NIRS data sets. *Chemometr Intell Lab.* 2010;101(2):87-94.
24. Allegrini F, Fernández Pierna JA, Fragoso WD, Olivieri AC, Baeten V, Dardenne P. Regression models based on new local strategies for near infrared spectroscopic data. *Anal Chim Acta.* 2016;933:50-58.
25. Filzmoser P, Liebmann B, Varmuza K. Repeated double cross validation. *J Chemometrics: A Journal of the Chemometrics Society.* 2009;4(23):160-171.
26. Davrieux F, Dufour D, Dardenne P, et al. LOCAL regression algorithm improves near infrared spectroscopy predictions when the target constituent evolves in breeding populations. *J Near Infrared Spec.* 2016;24(2):109-117.
27. Williams PC. Implementation of near-infrared technology. In: Williams P, Norris KH, eds. *Near-Infrared Technology in the Agricultural and Food Industries.* St. Paul, Minnesota, USA: American Association of Cereal Chemist; 2001:145-169.
28. Cozzolino D, Morón A. Potential of near-infrared reflectance spectroscopy and chemometrics to predict soil organic carbon fractions. *Soil Tillage Res.* 2006;85(1-2):78-85.

SUPPORTING INFORMATION

Additional supporting information may be found online in the Supporting Information section at the end of the article.

How to cite this article: Shen G, Lesnoff M, Baeten V, et al. Local partial least squares based on global PLS scores. *Journal of Chemometrics.* 2019;e3117. <https://doi.org/10.1002/cem.3117>